Supporting information: Sub-Nanosecond Secondary Geminate Recombination in Mercury Halides HgX_2 (X = I, Br) Investigated by Time-Resolved X-ray Scattering

Denis Leshchev[a†], Dmitry Khakhulin[b], Gemma Newby[a], Hosung Ki[c, d], Hyotcherl Ihee[c, d], Michael Wulff[a*]

[a] European Synchrotron Radiation Facility, 71 Avenue des Martyrs, 38000 Grenoble, France

[b] European XFEL GmbH, Holzkoppel 4, D-22869 Schenefeld, Germany

[c] Center for Nanomaterials and Chemical Reactions, Institute for Basic Science (IBS), Daejeon 305-701, Korea

[d] Department of Chemistry and KI for the BioCentury, Korea Advanced Institute of Science and Technology (KAIST), Daejeon 305-701, Korea

*To whom correspondences should be addressed

† Current address: Department of Chemistry, Northwestern University, Evanston, Illinois 60208, USA

Supplementary note S1. Determination of the main reaction pathway for HgX_2

The structural parameters of the HgX_2 molecules used for calculation of the scattering signals were taken from the published works[1,2] and are summarized in Table S1.

To determine the main reaction pathway of HgX_2, we fitted the data recorded at various time delays with candidate structures and compared the goodness of fit. The theoretical scattering signals were calculated using the following equation:

$$\Delta S_{theory}(q,t) = \gamma(t)\Delta S_{solute}(q) + \Delta T(t)\left(\frac{\delta S(q)}{\delta T}\right)_V + \Delta\rho(t)\left(\frac{\delta S(q)}{\delta \rho}\right)_T \quad (1)$$

where q and t are transferred momentum and measured time delay; $\Delta S_{theory}(q,t)$ is the theoretical signal; $\gamma(t)$ is the excited state fraction; $\Delta S_{solute}(q)$ is the difference scattering calculated for the solute using Debye formula; $\Delta T(t)$ and $\Delta\rho(t)$ are the temperature rise and density change, respectively; $\left(\frac{\delta S(q)}{\delta T}\right)_V$ and $\left(\frac{\delta S(q)}{\delta \rho}\right)_T$ are the short- and long term solvent heating response differentials measured separately using azo-dye compounds.[3] We note that the solute-solvent cross term (cage term) was not considered in this work because its contribution is small as discussed below (Note S3). In the model, the calculated theoretical $\Delta S_{solute}(q)$ was corrected for polychromaticity of the x-ray pink spectrum using standard procedures.[4]

The data is fitted using a standard χ^2 estimator determined as

$$\chi^2 = \sum_q \left(\frac{\Delta S_{exp}(q,t) - \Delta S_{theory}(q,t)}{\sigma(q,t)}\right)^2 \quad (2)$$

where $\Delta S_{exp}(q,t)$ and $\sigma(q,t)$ are the measured experimental signal and standard errors of the signal. To evaluate the models' quality of fit, we used reduced χ^2_{red}=$\chi^2/(N-p-1)$ with N being the number of q points and p being the number of fitted parameters.

The resulting fits and corresponding χ^2_{red} are shown in Figures S1 and S2 for HgI_2 and $HgBr_2$, respectively. For HgI_2 and $HgBr_2$ the chosen time delays are 70 ps and 60 ps, respectively, where the TRWAXS signal is at maximum. We tested four possible channels: (1) two-body dissociation resulting in formation of the HgX and X radicals, (2) three-body dissociation resulting in formation of the Hg and two X radicals, (3) direct formation of molecular X_2 along with the Hg radical, (4) formation of an isomer HgX-X. Additionally, for $HgBr_2$, we consider the possibility of undergoing a mixture of two- and three-body dissociations. In the case of HgI_2, we find that the two-body dissociation model fits the data significantly better than models involving the other channels. In the case of $HgBr_2$, we find that using a combination of two- and three-body dissociation channels provide the best fit. These results are in a good agreement with the previous TRWAXS studies.[1,2]

Table S1. Structural parameters of HgX_2 and its potential photoproducts from previous works[1,2] and from TRWAXS refinement in this work. The experimental values are marked (exp).

Channel	Hg-X (Å)	X-X (Å)	X-Hg-X (deg)	Hg-X-X (deg)
HgI_2	2.587 2.60 ± 0.01 (exp)	5.174 5.02 ± 0.02 (exp)	180.0 150 ± 2 (exp)	-
HgI-I	2.799	2.893	-	180.0
HgI+I	2.814 2.80 ± 0.02 (exp)	-	-	-
$Hg+I_2$	-	2.669	-	-
Hg+2I	-	-	-	-
$HgBr_2$	2.405 2.44 ± 0.04 (exp)	4.810 4.85 ± 0.10 (exp)	180.0 160 ± 20 (exp)	-
HgBr-Br	2.573	2.600	-	180.0
HgBr+Br	2.625 2.69 ± 0.07 (exp)	-	-	-
$Hg+Br_2$	-	2.286	-	-
Hg+2Br	-	-	-	-

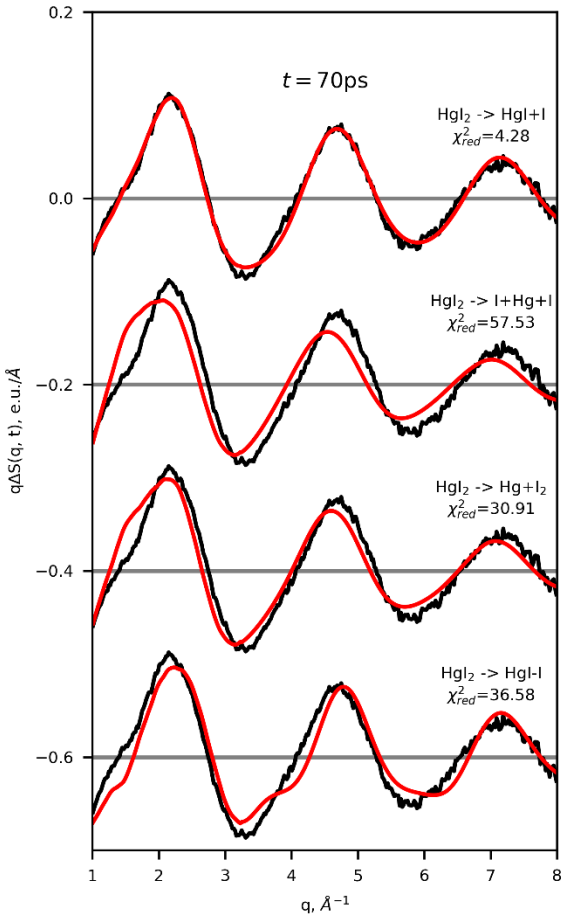

Figure S1. Comparison of structural signals with the experimental data recorded for HgI_2 in acetonitrile at 70 ps.

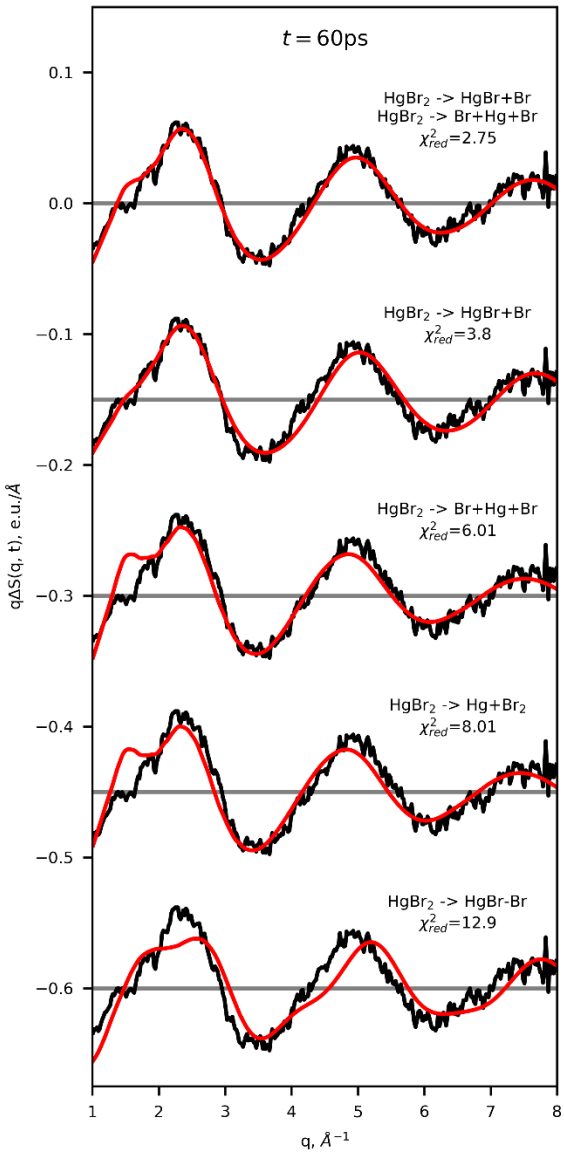

Figure S2. Comparison of structural signals with the experimental data recorded for $HgBr_2$ in acetonitrile at 60 ps.

Supplementary note S2. Structural refinement using TRWAXS.

To further assess the structures of ground state HgX_2 and the photodissociated HgX radicals, we performed a structural fitting of the data. To avoid potential contributions from the cage, albeit small, we confined the fitting to the high-q part of the data, $q \geq 4$ Å^{-1}. Using the structural parameters from Table S1 as starting values, we fitted theoretical TRWAXS signals to the data. The fits are shown in Figure S3 and the resulting best fit parameters are summarized in Table S1. For HgI_2 we find that the ground state

converges to a symmetric geometry with the HgI bond length in good agreement with previous calculations. The I-Hg-I angle, on the other hand, converges to ~150°, which deviates from the expected linear geometry. Similarly, the refined structure of $HgBr_2$ gives a symmetric molecule with a HgBr bond length in agreement with calculations and with an Br-Hg-Br angle of 160°. The angle is statistically insignificantly different from the linear geometry due to limited signal-to-noise ratio of the data. Finally, we find that the HgX bond length for the excited state photofragments are also in fair agreement with calculations.

We note that calculations predict linear equilibrium geometry for mercury halides;[1,2] however, bending vibrations are known to "shrink" the distance between the terminal atoms in triatomic molecules, which has been observed in electron diffraction,[5–7] as well as in spectroscopic measurements.[8] While we intend to investigate the origin of the apparent bending in the future, we find that the bending angle of the ground state geometry have little to no effect on the recombination kinetics of the HgX/X radicals, which is the focus of this work.

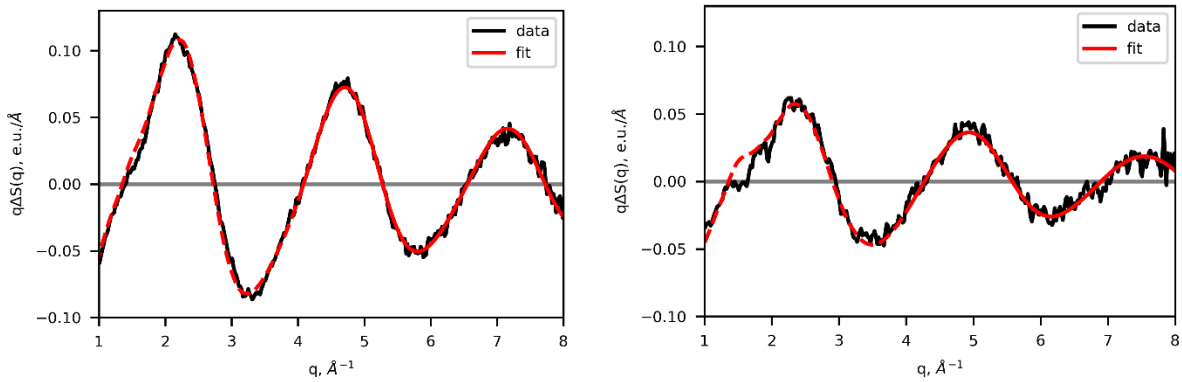

Figure S3. Structural fitting of HgI_2 (left) and $HgBr_2$ (right) data recorded at 70 and 60 ps, respectively. Solid red lines show the fits for $q \geq 4$ Å^{-1} and the dashed lines show the extrapolation to low-q.

Supplementary note S3. Cage contribution effect.

In previous work we demonstrated that the cage contribution can be obtained from the residuals of the fit from the high-q part of the data using naked solute structures and solvent heating.[9] In this way we extrapolated the curves to lower q, $q < 4$ Å^{-1} (Figure S3, see red dashed lines), and obtained the cage term as the difference between the data and the model curve (Figure S4). We note that the cage contribution extracted this way represents the highest limiting signal for a possible cage term, since it also includes a possible fitting uncertainty of the selected structural model to the experimental data in the low-q region.

An estimate the effect of the cage contribution on the transient species concentrations, is done as follows. For HgI_2, the cage signal is confined to $1 < q < 3.5$ $Å^{-1}$ with the maximum amplitude constituting ~10 % of that for the solute. Since the cage signal is affecting a third of the data recorded at low-q below 3.5 $Å^{-1}$, the effect on the parameter fitting in the entire q-range up to 8 $Å^{-1}$ is at most a third of the maximum cage amplitude, i.e. about 3-4%. In the case of $HgBr_2$, the estimated cage contribution is about 20%, while being confined to q values below 2.5 $Å^{-1}$, i.e. affecting only 20% of the data, which will result in the maximum bias of ~4%. In both cases, the effect of the cage on the concentrations is well within the general uncertainty in the analysis (see main text), and it can therefore safely be omitted.

We note that the cage contribution is "slaved" to the solute changes, i.e. changes in tandem with the solute concentration. Therefore omission of the cage may affect the total concentrations of the transient species, but will not affect their time dependence.

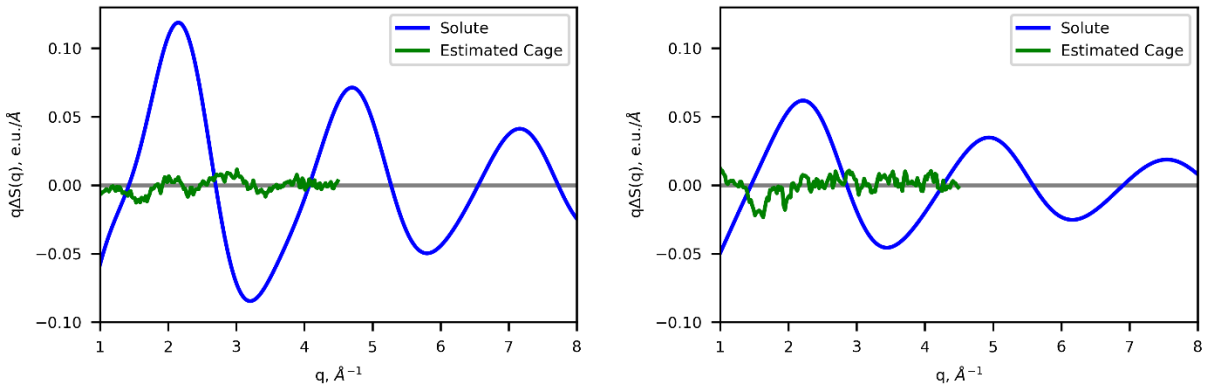

Figure S4. Estimation of the cage contribution in acetonitrile solution for HgI_2 (left) and $HgBr_2$ (right) recorded at 70 and 60 ps, respectively.

Supplementary note S4. Differential equations used to describe NGR channel.

For HgI_2, the time-dependent concentration of the radicals undergoing NGR channel was obtained by numerically solving the following system of equations:

$$\frac{\partial C_{HgI_2}(t)}{\partial t} = K_{HgI+I\rightarrow HgI_2} C_{HgI}(t) C_I(t)$$

$$\frac{\partial C_{HgI}(t)}{\partial t} = -K_{HgI+I\rightarrow HgI_2} C_{HgI}(t) C_I(t)$$

$$\frac{\partial C_I(t)}{\partial t} = -K_{HgI+I\rightarrow HgI_2} C_{HgI}(t) C_I(t) - 2K_{I+I\rightarrow I_2} C_I^2(t)$$

$$\frac{\partial C_{I_2}(t)}{\partial t} = K_{I+I\rightarrow I_2} C_I^2(t)$$

Where C represents the concentration of respective species and K is the bimolecular recombination coefficient of the respective pair of species. The system was solved with a the following set of initial conditions: $C_{HgI_2}(0) = -C_0$, $C_{HgI}(0) = C_0$, $C_I(0) = C_0$, $C_{I_2}(0) = 0$, with C_0 being the initial concentration of the species that undergo NGR.

Similarly, for $HgBr_2$, the following system of equations was used:

$$\frac{\partial C_{HgBr_2}(t)}{\partial t} = K_{HgBr+Br\rightarrow HgBr_2} C_{HgBr}(t) C_{Br}(t)$$

$$\frac{\partial C_{HgBr}(t)}{\partial t} = -K_{HgBr+Br\rightarrow HgBr_2} C_{HgBr}(t) C_{Br}(t) + K_{Hg+Br\rightarrow HgBr} C_{Hg}(t) C_{Br}(t)$$

$$\frac{\partial C_{Br}(t)}{\partial t} = -K_{HgBr+Br\rightarrow HgBr_2} C_{HgBr}(t) C_{Br}(t) - 2K_{Br+Br\rightarrow Br_2} C_{Br}^2(t) - K_{Hg+Br\rightarrow HgBr} C_{Hg}(t) C_{Br}(t)$$

$$\frac{\partial C_{Br_2}(t)}{\partial t} = K_{Br+Br\rightarrow Br_2} C_{Br}^2(t)$$

$$\frac{\partial C_{Hg}(t)}{\partial t} = -K_{Hg+Br\rightarrow HgBr} C_{Hg}(t) C_{Br}(t)$$

The initial conditions were set to $C_{HgBr_2}(0) = -C_0$, $C_{HgBr}(0) = xC_0$, $C_{Br}(0) = (2-x)C_0$, $C_{Br_2}(0) = 0$, $C_{HgBr}(0) = (1-x)C_0$, with x being the fraction of radicals undergoing two-body dissociation.

Supplementary note S5. Thermodynamic analysis of the photoreactions.

The time dependent changes in the temperature and the density were determined together with the changes in the concentrations of the transient species, as discussed in the main text. The retrieved changes in the thermodynamic variables are shown in Figure S5. In case of HgI_2, the final temperature change observed at 1 μs is 0.36 ± 0.02 K, which is higher than 0.18 K predicted solely based on the recombination of the species observed in the present experiment. Therefore, the additional temperature must come from the photofragments that relax inside the cage via PGR, as well as from the excited HgX_2* molecules that decay via internal conversion directly into vibrationally hot HgX_2 and then cool down vibrationally.

To calculate the fraction of the molecules undergoing in-cage recombination, we can use the standard formula:

$$C_{PGR} = T_{offset}\left[\frac{V_{mol}N_A}{C_P}h\nu\right]^{-1}$$

where T_{offset} is the difference between observed and expected temperatures at 1 μs, V_{mol} is molar volume of acetonitrile, N_A is the Avogadro number, C_V is

We predict that 0.65 ± 0.1 mM undergo this channel. Similarly, in case of $HgBr_2$, the observed change in the temperature at 1 μs is 0.38 ± 0.04 K, which is higher compared to predicted 0.15 K. Therefore, we estimate that about 0.8 ± 0.3 mM have recombined/relaxed in-cage.

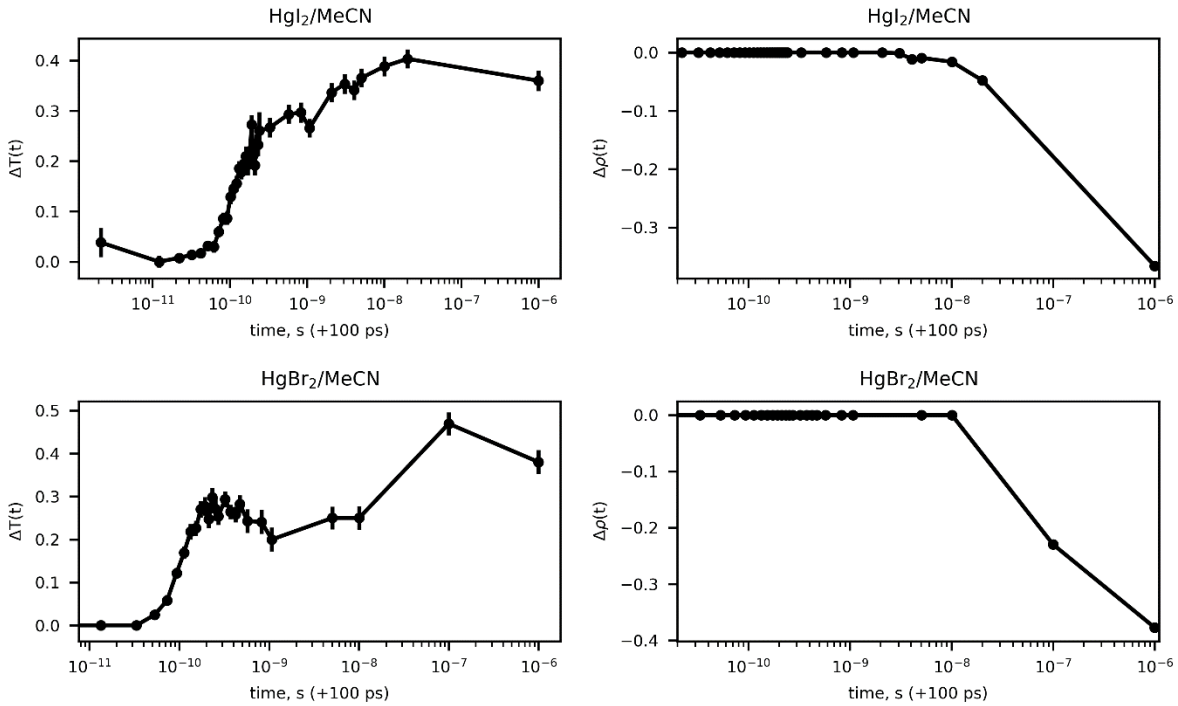

Figure S5. Changes in temperature in K (HgI_2 – top-left, $HgBr_2$ – bottom-left) and in density in kg/m^3(HgI_2 – top-right, $HgBr_2$ – bottom-right) as a function of time, as determined from the fitting of the TRWAXS data.

Supplementary note S6. The effect of the instrument response function (IRF) on the TRWAXS analysis.

The finite temporal resolution of the TRWAXS measurements, arising from the the ca. 100 ps long x-ray pulse from the ESRF synchrotron, results in smearing of the kinetic data recorded around time-zero. Therefore, to correctly estimate the rates and yields of the recombination processes, especially the SGR channel, it is important to include the IRF in the kinetic fitting. The effectiveness of this procedure is determined by the accuracy of the IRF characterization. In our study, we used the IRF from streak camera measurements of the x-ray pulse temporal profiles, i.e. the asymmetric gaussian shape (see below).5 While these measurements provide a good estimate of the IRF, we note that the current in the synchrotron ring was decaying throughout the multi-hour measurement of the TRWAXS data, which directly affected the x-ray pulse shape and duration used for collecting the individual repetitions of the data collection. Due to these changes, the effective IRF that is reflected in the averaged data may deviate from the temporal profile measured by the streak camera. Therefore, the accuracy of the estimates concerning the SGR process are limited by the accuracy of the IRF used for fitting, which may be responsible for the factor of 2 difference in the obtained SGR yields from TRWAXS and OTA.

Supplementary note S7. Time scale of the inter-radical distance distribution broadening for the HgI/I radical pair.

In the simplest case, following the photolysis the radicals are separated by a well-defined distance corresponding to several solvent molecules. As the time progresses, the radicals diffuse through the solvent causing the inter-radical distance to broaden. The concentration of radicals at a specific distance d as a function of time t can be derived from the diffusion equation and is expressed as

$$C(d,t) = \frac{C_0}{(4\pi Dt)^{3/2}} \exp\left(-\frac{(d-d_0)^2}{4Dt}\right)$$

with d_0 being the initial separation distance and D being the relative diffusion constant. The time-dependent FWHM of the inter-radical distance distribution can then be expressed as

$$FWHM \approx 2.355\sqrt{2Dt}$$

The relative diffusion constant D for the HgI/I pair of radicals is related to bimolecular recombination rate $K_{HgI+I\rightarrow HgI_2}$ as[12]

$$K_{HgI+I\rightarrow HgI_2} = 2\pi DR$$

where R is the encounter distance at which reaction occurs instantaneously. Assuming the encounter distance $R = 6$ Å, i.e. the approximate size of the parent molecule cavity, and using the obtained in this work $K_{HgI+I\rightarrow HgI_2} = 6.5 \times 10^{10} M^{-1}s^{-1}$, we estimate $D = 2.8 \times 10^{-4}\ cm^2/s$. From this we obtain that the time required for the FWHM of distance distribution to broaden up to 10 Å is $t \approx 3\ ps$.

References

1 T. K. Kim, M. Lorenc, J. H. Lee, M. Lo Russo, J. Kim, M. Cammarata, Q. Kong, S. Noel, A. Plech, M. Wulff and H. Ihee, *Proc. Natl. Acad. Sci.*, 2006, **103**, 9410–9415.

2 S. Jun, J. H. Lee, J. Kim, J. Kim, K. H. Kim, Q. Kong, T. K. Kim, M. Lo Russo, M. Wulff and H. Ihee, *Phys. Chem. Chem. Phys.*, 2010, **12**, 11536.

3 K. S. Kjær, T. B. van Driel, J. Kehres, K. Haldrup, D. Khakhulin, K. Bechgaard, M. Cammarata, M. Wulff, T. J. Sørensen and M. M. Nielsen, *Phys. Chem. Chem. Phys.*, 2013, **15**, 15003–15016.

4 H. Ihee, M. Wulff, J. Kim and S. Adachi, *Int. Rev. Phys. Chem.*, 2010, **29**, 453–520.

5 Y. Morino, *Acta Crystallogr.*, 1960, **13**, 1107.

6 Y. Morino, J. Nakamura and P. W. Moore, *J. Chem. Phys.*, 1962, **36**, 1050.

7 G. Nagarajan, *J. Mol. Spectrosc.*, 1964, **13**, 361–392.

8 G. Winterhoff, S. C. Galleguillos Kempf, P. Jensen and P. R. Bunker, *J. Mol. Spectrosc.*, 2018, **354**, 71–82.

9 D. Khakhulin, L. M. Lawson Daku, D. Leshchev, G. E. Newby, M. Jarenmark, C. Bressler, M. Wulff and S. E. Canton, *Phys. Chem. Chem. Phys.*, 2019, **21**, 9277–9284.

10 L. Guerin, Q. Kong, D. Khakhulin, M. Cammarata, H. Ihee and M. Wulff, *Synchrotron Radiat. News*, 2012, **25**, 25–31.

11 K. Haldrup, T. Harlang, M. Christensen, A. O. Dohn, T. B. van Driel, K. S. Kjær, N. Harrit, J. Vibenholt, L. Guerin, M. Wulff and M. M. Nielsen, *Inorg. Chem.*, 2011, **50**, 9329–9336.

12 R. M. Noyes, *Progr. React. Kinet.*, 1961, **1**, 129.